The Ocular Surface 38 (2025) 230–241

Contents lists available at ScienceDirect

The Ocular Surface

journal homepage: www.elsevier.com/locate/jtos

Exploration of imaging and molecular biomarkers for differentiation of neuropathic corneal pain from dry eye syndrome

Jun Cheng [a,b,c], Chang Liu [d,e], Mingyi Yu [d,e], Isabelle Xin Yu Lee [d], Xinyue Wang [f], Victor Wei-Tse Hsu [d], Aya Takahashi [d], Jodhbir S. Mehta [d,e,g,h], Lei Zhou [i,j], Louis Tong [g,h,k], Yu-Chi Liu [d,e,g,h,l,*]

[a] Eye Institute of Shandong First Medical University, Qingdao Eye Hospital of Shandong First Medical University, China
[b] State Key Laboratory Cultivation Base, Shandong Provincial Key Laboratory of Eye Disease, China
[c] School of Ophthalmology, Shandong First Medical University, China
[d] Tissue Engineering and Cell Therapy Group, Singapore Eye Research Institute, Singapore
[e] Cornea and Refractive Surgery Group, Singapore Eye Research Institute, Singapore
[f] School of Optometry, The Hong Kong Polytechnic University, Hong Kong
[g] Department of Cornea and External Eye Disease, Singapore National Eye Centre, Singapore
[h] Ophthalmology and Visual Sciences Academic Clinical Program, Duke-NUS Medical School, Singapore
[i] School of Optometry, Department of Applied Biology and Chemical Technology, Research Centre for SHARP Vision (RCSV), The Hong Kong Polytechnic University, Hong Kong
[j] Centre for Eye and Vision Research (CEVR), 17W Hong Kong Science Park, Hong Kong
[k] Ocular Surface Research Group, Singapore Eye Research Institute, Singapore
[l] Department of Ophthalmology, National Taiwan University, Taiwan

ARTICLE INFO

Keywords:
Neuropathic corneal pain
Dry eye diseases
In-vivo confocal microscopy
Tear proteomics
Microneuromas

ABSTRACT

Purpose: To investigate the imaging, clinical, and tear proteomic profiles between neuropathic corneal pain (NCP) and dry eye disease (DED), and to identify potential imaging and molecular biomarkers for the differentiation of NCP from DED.

Methods: This cross-sectional study included 54 NCP patients (105 eyes), 53 DED patients (106 eyes), and 54 healthy controls (108 eyes). All subjects were evaluated with ocular surface assessment, ocular pain assessment survey (OPAS), and in-vivo confocal microscopy to characterize corneal nerves, microneuromas (MNs), immune cells, and epithelial cells. Tear quantitative proteomics were analyzed.

Results: The percentage of presence of MNs, the number, total area, total perimeter, and average area of MNs were significantly higher in the NCP group than the other two groups. NCP patients had significantly higher corneal nerve fiber width. MNs parameters were significantly correlated with the OPAS scores ($r = 0.20$ to 0.48, all $P < 0.05$). Particularly, in peripheral NCP, both MNs total area and perimeter exhibited a significant correlation with the OPAS eye pain intensity ($r = 0.55$–0.57, both $P < 0.05$). Combinations of MNs parameters and OPAS scores had high diagnostic efficacy for NCP with an area under the curve (AUC) of 0.916. A total of 129 significantly differential proteins were identified, such as up-regulated vinculin and down-regulated DLG associated protein 4 in NCP, as well as up-regulated S100A12 and matrix metallopeptidase 9 in DED. These dysregulated proteins were linked to neuron apoptosis, inflammatory response, and synaptic transmission.

Conclusion: NCP patients present with different imaging features, clinical characteristics and proteomic profiles, compared with DED patients. These can be used as differentiating indicators.

1. Introduction

Neuropathic pain is caused by peripheral nerve injury or changes in pain processing in the central nervous system [1]. When this phenomenon occurs in the cornea, it is referred to as neuropathic corneal pain (NCP), which presents as ocular pain, hyperalgesia, burning sensation, and photophobia. NCP significantly affects the quality of life (QoL) [2,3]. The etiology of NCP includes systemic diseases, such as diabetes, small fiber neuropathy, or systemic autoimmune

* Corresponding author. Singapore National Eye Centre, The Academia, 20 College Road, Discovery Tower, Level 6, 169856, Singapore.
E-mail address: liuchiy@gmail.com (Y.-C. Liu).

https://doi.org/10.1016/j.jtos.2025.08.002
Received 26 December 2024; Received in revised form 9 August 2025; Accepted 12 August 2025
Available online 14 August 2025

Abbreviations

NCP	neuropathic corneal pain
DED	dry eye disease
MNs	microneruomas
OPAS	Ocular Pain Assessment Survey questionnaire
OSDI	ocular surface disease index
IVCM	in-vivo confocal microscopy
QoL:	quality of life
CNFD	corneal nerve fiber density
CNBD	corneal nerve branch density
CNFL:	corneal nerve fiber length
CTBD	corneal total branch density
CNFA	corneal nerve fiber area
CNFW	average width of corneal nerves fibers
CFracDim	fractal dimension for nerves fibers

diseases, as well as ocular causes like refractive surgery, herpes simplex keratitis and dry eye [4-6]. Using in-vivo confocal microscopy (IVCM), several studies have identified alterations in the cornea microstructure in NCP, including reduced corneal nerve fiber density (CNFD), increased microneuromas (MNs) and immune cells, as well as activation of the stromal keratocytes [7-9]. The pathogenesis of NCP involves a cascade of neuromediators, inflammatory factors, and neuropeptides, contributing to intricate pathogenesis associated with neuroinflammation, wound healing, neurotoxicity, neutrophil degeneration, and apoptosis signaling pathways [9,10]. Currently, there is no consensus on the diagnosis of NCP, and the diagnosis of NCP is primarily based on clinical features and symptoms [11]. However, there are often overlapping symptoms between NCP and dry eye disease (DED), and there is no objective biomarker available to differentiate NCP from DED.

DED is multifactorial and encompasses a combination of symptoms of ocular dryness, burning sensation, tenderness, and aching, which overlap with those of NCP [12]. The clinical manifestations include meibomian gland obstruction or atrophy, and ocular surface staining on the cornea or conjunctiva. Morphologically, DED patients present with reduced corneal nerve density [13], presence of nerve beading or neuromas [14,15], increased nerve diameter and tortuosity, and increased immune cells on IVCM [16-18]. The pathogenesis is associated with the dysregulation of multiple inflammatory mediators [19], triggering neurogenic inflammation and leading to a vicious cycle of DED [20]. Given the similarity of parts of the symptomatology and pathogenesis, the treatment for NCP and DED, such as lubricants and anti-inflammatory agents [21-23], also overlap. However, a considerable proportion of NCP patients are refractory to conventional dry eye treatment [11]. Furthermore, central type of NCP requires systemic pharmacotherapy for the alleviation of the symptoms [24]. These underscore the importance of differentiation between these 2 conditions to deliver more effective treatment.

Tear proteomics is a reliable approach for understanding the causative mechanism and biochemical changes in ocular surface diseases. Several studies have investigated the tear proteomics of DED [25]. Our group has also for the first time characterized the tear proteomic profiles and associated biological pathways in NCP [9]. However, there is currently no existing literature comparing the molecular profiles between NCP and DED, which may open an avenue to identify potential molecular biomarkers to distinguish these two conditions.

Researchers have been attempting to identify the differences between NCP and DED in corneal nerve imaging. Moein [8] observed that MNs were only present in NCP patients but not in DED, suggesting that MNs could serve as a specific diagnostic marker for NCP. However, another study found that MNs can be present in 21.8 % of DED patients [15]. This suggests that the presence of MN alone may not have sufficient diagnostic ability for NCP. Clinicians would need more precise diagnostic parameters that can reflect the symptoms and signs of NCP.

In this study, we investigated and compared the corneal IVCM imaging characteristics, ocular surface objective and subjective assessments, and tear proteomics among NCP, DED, and control subjects. We aimed to identify potential imaging or proteomic diagnostic panels to distinguish NCP from DED.

2. Methods

2.1. Study design and patients

This cross-sectional, comparative study was conducted in Singapore National Eye Centre and Singapore Eye Research Institute. Approval for the study was granted by the Institutional Review Board of SingHealth (number 2022/2046), Singapore. The study was conducted in accordance with the Declaration of Helsinki, and informed consent was obtained from all the subjects.

There is currently no consensus in the diagnostic criteria for NCP, and we used the published inclusion criteria for the present study [2,9,26]: (1) Persistent (>3 months) ocular pain or pain-like symptoms such as burning sensation, allodynia, light sensitivity, or hyperalgesia, with scores at least 30 % on more than three questions in the Ocular Pain Assessment Survey (OPAS) questionnaire; (2) Abnormalities in corneal nerves such as MN formation, beading pattern, nerve tortuosity, reduction of CNFD, or corneal nerve fiber length (CNFL) on IVCM evaluation; and (3) Minimal ocular surface staining, with National Eye Institute (NEI) dot-count scores less than 2 [9,27]. The type of NCP was categorized based on the proparacaine challenge test: patients who experienced complete relief after topical proparacaine administration suggested peripheral NCP, while those who experienced partial relief or no response indicated mixed and central NCP, respectively [3].

DED was diagnosed based on the Dry Eye Workshop II criteria: an ocular surface disease index (OSDI) score $\geq$13, and tear break-up time (TBUT) < 10 second or presence of ocular surface staining (>5 corneal spots, >9 conjunctival spots, or lid margin >2 mm length and >25 % in width) [28].

The control group consisted of healthy individuals who were age- and sex-matched, had no history of ocular or systemic diseases, or ocular surgery, and did not use topical eye drops. Patients with active ocular surface disease and concomitant ocular diseases such as uveitis or other ocular inflammation that could potentially induce ocular pain, were also excluded.

2.2. IVCM scans and images analysis for corneal nerves, microneuromas, epithelial cells, and immune cells

Corneal nerve plexus, MNs, epithelial cells, and immune cells were evaluated using IVCM (Heidelberg Retina Tomography III, Rostock Cornea Module, Heidelberg Engineering GmbH). Scanning was performed at the central cornea and four areas positioned 3 mm above, below, nasal and, temporal to the apex of the cornea. The scanning depth encompassed from the corneal epithelium to the endothelium. The corneal nerve plexus was analyzed using the ACCMetrics software (University of Manchester) [29]. A total of 25 well-focused images were chosen from these five regions (five images per region with each trunk nerve and branch nerve being selected only once). The following parameters were obtained: CNFD (fibers/mm^2 with an area per frame = 0.16033 mm^2), corneal nerve branch density (CNBD; branch points on main fibers/mm^2), CNFL (total length of fibers mm/mm^2), corneal total branch density (CTBD; total number of branch points/mm^2), corneal nerve fiber area (CNFA; total nerve fiber area mm^2/mm^2), corneal nerve fiber width (CNFW; width of nerves fibers mm/mm^2) and corneal nerve fiber fractal dimension (CFracDim). CFracDim represents a spatial loss in nerve distribution, with higher CFracDim values indicating a more uniform nerve distribution.

MNs were defined as focal swellings of nerves characterized by relatively large, diffuse, and bright areas arising from the nerves [30]. All images containing MNs were selected, and the same MN was only selected once. These MNs were analyzed using ImageJ software (National Institutes of Health, MD). The area of each MN was quantified, and the number of all MNs was counted. Total MN area (μm^2) and total MN perimeter (μm) represented the cumulative sum from all the images for their respective measurements. Average MN area (μm^2) and average perimeter (μm) indicated the mean values calculated from all the images.

The AIConfocal Rapid Image Evaluation System (ARIES; ADCIS, S.A., Saint-Contest, France) was used for the analysis of the corneal epithelial cells and immune cells. For each eye, five best-focused images of the corneal epithelium were selected to obtain the following parameters: epithelial cell count, cell density (cells/μm^2), average cell size (μm^2), and cell circularity. Immune cells were defined as small white cells that separate from or connect to the nerve branches [31]. Ten representative images were chosen per eye, and the following parameters were obtained: cell density (cells/μm^2), average length (μm), average area (μm^2), and elongation (the absolute value of the difference between the major and minor axis divided by the sum of the major and minor axis).

2.3. Ocular surface objective and subjective assessments

The Schirmer's I test, TBUT, Oxford and NEI scores were performed with the published protocols [32]. Assessment of the ocular surface and corneal integrity was performed using the Oxford score (0–5) [33] and NEI scale (0–15), respectively [34].

The OSDI questionnaire assesses the symptoms of dry eye (Q1-5), its impact on vision-related functioning (Q6-9), and the effect of environmental factors (Q10-12). The total OSDI score was then calculated as: OSDI = [(sum of scores for all questions answered) × 100]/[(total number of questions answered) × 4] [35]. The OPAS questionnaire is a validated multidimensional tool comprising six dimensions: eye pain intensity in the past 24 h, eye pain intensity in the last 2 weeks, non-ocular pain intensity, QoL assessment, aggravating factors, and associated factors examination. Participants rated their responses on a numerical scale ranging from 0 to 10 [36].

2.4. Tear proteomic profiles analysis

Tear proteomic quantitative analysis was conducted with the protocol described previously [9,37,38]. The Schirmer strips were mixed with 100 μL lysis buffer and incubated. The Bio-Rad DC Protein assay was utilized to measure the total protein concentration. The tear proteins eluted were subjected to reduction, alkylation, trypsin digestion, and desalting processes. Subsequently, the quantification of the total peptide quantities was performed. All peptide samples underwent analysis by an Orbitrap Exploris™ 480 Mass Spectrometer using an EASY-Spray™ Source alongside an EASY-nLC 1200 system. The separation of liquid chromatography was conducted by employing an Acclaim PepMap 100C18 as a pre-column and a PepMap®RSLC C18 as an analytical column. A library-independent direct data-independent acquisition (DIA) workflow was employed to process the DIA data using Spectronaut 15 from Biognosys. Raw protein abundance values were derived after fragment ions were selected for quantification based on the default quality control criteria as implemented in the map DIA. The downstream data analysis, data visualization, and Gene Ontology term enrichment were performed using custom scripts in R (version 4.1.1) software. The raw abundance data were median normalized and log-transformed for all the statistical analyses. Significant differentially expressed proteins were identified using the threshold of Wilcoxon Rank-Sum Test $p < 0.05$ and $|\log_2 FC| > 0.585$. Partial Least Squares Discrimination Analysis (PLS-DA) was used to discriminate the proteomic profiles between NCP and DED. PLS-DA is a robust method for projecting and analyzing the data structure by maximizing the differences between the groups according to the predefined classification and identifying the influencing variables that cause the differences between the groups.

2.5. Statistical analysis

The normality of data distribution was assessed using the Kolmogorov-Smirnov test. Continuous variables were reported as mean ± standard deviation. One-way analysis of variance (ANOVA) was used to analyze normally-distributed data, followed by Tukey's multiple tests for pairwise comparisons. Non-normally distributed data were analyzed using a Kruskal-Wallis H test, with a Dunnett's T3 test for pairwise comparisons. Chi-square test was used to compare the categorical variables. Spearman's rank order correlation analysis examined the associations between the MN or corneal nerve parameters, and questionnaire scores. For the ocular surface objective parameters and IVCM parameters, the average of both eyes were used for the correlation analysis with the OPAS and OSDI scores which were patient-based, rather than eye-based scores. Receiver operating characteristic curve analysis examined the diagnostic performance of the use of objective parameters for NCP from the DED. Areas under the curves (AUCs) were calculated as measures of the accuracy of the tests. Cutoff point, sensitivity, specificity, positive predictive value and negative predictive value were also calculated. The required sample size was calculated based on type I error at 0.05, type II error at 0.20, confidence level at 0.95, the ratio of NCP and DED patients at 1/1, and expected AUC at 0.90 [39]. Hence, 51 patients was required for each arm. A P value < 0.05 was considered statistically significant. Statistical analyses were performed using GraphPad Prism 9.3.0 (GraphPad software, La Jolla, California, USA).

3. Results

3.1. Demographic information and comorbidities

A total of 54 patients (105 eyes) with NCP, 53 patients with DED (106 eyes), and 54 healthy volunteers (108 eyes) were included in the study. The average age of the NCP, DED, and control groups was 55.7 ± 14.0, 59.6 ± 14.8, and 54.1 ± 15.2 years, respectively ($P = 0.143$). The study population was predominantly female, at 87.0 %, 75.5 % and 74.1 %, in the NCP, DED and control groups respectively ($P = 0.197$). In the NCP cohort, 33 eyes (31.4 %) had peripheral NCP, 24 eyes (22.9 %) had central NCP, and 48 eyes (45.7 %) presented with mixed NCP. Forty-five patients (83.3 %) in the NCP group had systemic comorbidities, with the most common being sleep disorders (38.9 %), followed by chronic pain syndrome (37.0 %). Twenty patients (37.0 %) had ocular comorbidities, of which 11 patients (20.4 %) had a history of refractive surgery. In the DED group, 43.4 % and 49.1 % had systemic comorbidities and ocular comorbidities, respectively (Table 1).

3.2. Ocular surface assessment and subjective symptoms

On OPAS evaluation, 37 NCP patients (68.5 %) complained of varying extents of eye pain in the last 24 h. Other commonly reported symptoms included burning sensation (53.7 %), photophobia (53.7 %), and tearing (40.7 %). In the DED group, a lower percentage of patients experienced these symptoms: 27.3 % presented with eye pain in the last 24 h 17.0 % of subjects exhibited burning sensation, 18.5 % complained of photophobia, and 20.8 % exhibited tearing. The mean scores of the six dimensions in NCP patients were significantly higher than those in DED and controls (all $P < 0.001$; Table 2). There was no significant difference between the DED and control group, except for the scores of the associated factors. The total OSDI score of the NCP group was also significantly higher compared to that of the DED and control groups (both $P < 0.001$; Table 2).

For the analysis of the three NCP subgroups, the mean scores of eye pain intensity for the last 24 h, non-eye pain intensity, QoL, aggravating

Table 1
Characteristics in NCP and DED patients.

Parameter	DED	NCP
Duration of disease (mean ± SD years)	3.7 ± 2.8	4.1 ± 5.2
Systemic comorbidities (n, %)		
Sleep disorder	3 (5.7)	21 (38.9)
Chronic pain syndrome	3 (5.7)	20 (37.0)
Migraine	1 (1.9)	8 (14.8)
Others	2 (3.8)	12 (22.2)
Anxious or depression	1 (1.9)	10 (18.5)
Rheumatoid arthritis	1 (1.9)	4 (7.4)
Sjogren syndrome	1 (1.9)	3 (5.6)
Dyslipidemia	7 (13.2)	3 (5.6)
Allergic disease (asthma, allergic rhinitis, atopic dermatitis and eczema)	5 (9.4)	5 (9.3)
Diabetes mellitus	1 (1.9)	3 (5.6)
Trigeminal neuralgia	0 (0)	2 (3.7)
Fibromyalgia	0 (0)	2 (3.7)
Meige syndrome	0 (0)	1 (1.9)
Anaemia	1 (1.9)	1 (1.9)
Remissioned leukemia	2 (3.8)	0 (0)
Crohn's disease	1 (1.9)	0 (0)
Thyroid disease	1 (1.9)	1 (1.9)
Ocular comorbidities (n, %)		
Refractive Surgery	7 (13.2)	11 (20.4)
Other ocular surgeries (cataract surgery, eyelid surgery, strabismus surgery)	18 (34.0)	6 (11.1)
Blepharospasm	1 (1.9)	6 (11.1)
Herpes zoster ophthalmicus	0 (0)	2 (3.7)
Systemic medications (n, %)		
No	47 (88.7)	35 (64.8)
Antihypertensive	1 (1.9)	1 (1.9)
Non-steroidal anti-inflammatory	1 (1.9)	3 (3.7)
Antitumor drugs	1 (1.9)	0 (0)
Anti-insomnia drugs	1 (1.9)	3 (3.7)
Gabapentin or Pregabalin	0 (0)	4 (7.4)
Antidepressants	0 (0)	5 (9.3)
Corticosteroids	0 (0)	2 (3.7)
Hydroxychloroquine	1 (1.9)	1 (1.9)
Topical medications (n, %)		
No	31 (58.5)	35 (64.8)
Artificial tears	3 (5.7)	5 (9.3)
Antihistamines	2 (3.8)	1 (1.9)
Corticosteroids	0 (0)	1 (1.9)
Cyclosporines	8 (15.1)	7 (13.0)
Diquafosol Sodium	9 (17.0)	6 (11.1)
Contact lenses history (n, %)		
Yes	12 (22.2)	17 (32.1)
No	42 (77.8)	36 (67.9)

factors, and associated factors in the mixed group exhibited higher values compared to those reported in the peripheral and central NCP groups. However, these differences did not reach statistical significance (Supplementary Table 1).

For ocular surface assessment, the NEI score in the NCP group was significantly lower than that in the DED group ($P < 0.001$) and comparable to that in the normal control group. The DED patients had significantly higher Oxford scores than the NCP patients ($P = 0.001$) and the controls ($P < 0.001$). There were no significant differences observed between the NCP group and DED group for the Schirmer's I results, both of which were significantly lower than that of the normal control group (all $P < 0.001$). Significant differences in the TBUT were observed among the three groups, with the DED group presenting with the lowest value, followed by the NCP group, and the control group (all $P < 0.0001$; Table 2).

3.3. IVCM findings for microneuromas, corneal nerves, immune cells, and epithelial cells

3.3.1. Microneuromas

Corneal MNs were present in all the NCP patients (100 %), with the proportion significantly higher than that of DED patients (58.5 %) and the controls (35.2 %), respectively ($P < 0.001$, Table 3). The mean number of MNs in the NCP group was significantly higher than that in the DED group and controls (both $P < 0.001$), while there was no significant difference between the control and DED groups (Table 3 and Fig. 1). The total area total perimeter, and average area of MNs in the NCP group were significantly larger than those in both the DED and control groups (all $P < 0.05$). There were no significant differences between the DED and the control group in all the MNs parameters. (Table 3, Fig. 1).

The number of MNs in the peripheral NCP (5.9 ± 3.0) and mixed NCP (6.3 ± 3.9) subgroups was significantly higher than that in the central NCP subgroup (3.8 ± 2.6) ($P = 0.036$ and $P = 0.012$ respectively), with no significant difference between peripheral and mixed NCP. There were no significant differences in the rest of the MNs parameters among the three subgroups.

3.3.2. Corneal nerves

NCP and DED patients had significantly lower CNFD, CNBD, CNFL, and CTBD than the controls, while these parameters were comparable between the NCP and DED groups. Of note, when comparing between the NCP and DED group, NCP patients had significantly higher CNFW than DED patients ($P = 0.036$). DED patients had significant lower CNFA ($P = 0.029$) and CFracDim ($P = 0.027$) than NCP patients. When comparing NCP and control group, the NCP patients had significantly higher CNFW ($P < 0.001$) and significantly lower CFracDim ($P = 0.017$; Table 3 and Fig. 2).

3.3.3. Immune cells

The immune cells elongation was significantly lower in the NCP and DED groups than in the controls ($P = 0.046$ and $P = 0.015$, respectively), indicating longer processes and smaller cell bodies which suggest more mature immune cells morphology. The immune cells density in the NCP and DED groups was significantly higher than that of the controls ($P = 0.003$), while no significant difference was observed between the NCP and DED groups. (Table 4, Fig. 3).

3.3.4. Corneal epithelial cells

Comparisons of basal epithelial cells among the three groups are presented in Table 4 and Fig. 3. The DED group had the highest cell density and smallest epithelial cell size than the NCP and control groups (all $P < 0.05$).

3.4. Correlation between subjective symptoms and imaging parameters

The scores of five dimensions of the OPAS questionnaire on the ocular symptoms were significantly and positively correlated with all the MNs parameters, including the number, total area, total perimeter, average area, and average perimeter of MNs ($r = 0.20$ to 0.49, all $P < 0.05$). The total OSDI scores presented with significant and positive correlation with all the MNs parameters ($r = 0.27$ to 0.44, all $P < 0.05$). The total OSDI scores also significantly and negatively correlated with the CNBD, CNFL, CTBD, and CFracDim ($r = -0.17$ to -0.19, all $P < 0.05$) (Table 5). There were significant and positive correlations between the CNFW and OSDI scores, as well as CNFW and eye pain intensity for the last two weeks and scores of associated factors on OPAS evaluation (all $P < 0.05$; Table 5).

We also specifically analyzed the correlation between the OPAS scores and imaging parameters for NCP patients. Negative correlations

Table 2
Subjective and objective assessment on ocular surface.

	Control	DED	NCP	*P* value	*P* values for post-hoc analysis		
					DED vs C	NCP vs C	NCP vs DED
Tear break-up time (Sec)	9.5 ± 2.0	2.1 ± 0.8	3.8 ± 2.6	**<0.0001**	**<0.0001**	**<0.0001**	**<0.0001**
Schirmer's I test (mm)	13.5 ± 7.9	7.1 ± 6.4	6.1 ± 5.1	**<0.0001**	**<0.0001**	**<0.0001**	0.611
Oxford score (0–5)	0.0 ± 0.1	0.6 ± 0.9	0.2 ± 0.5	**<0.0001**	**<0.0001**	**0.037**	**0.0001**
NEI score (0–15)	0.1 ± 0.3	2.0 ± 2.4	0.4 ± 0.6	**<0.0001**	**<0.0001**	0.336	**<0.0001**
OSDI	5.5 ± 9.5	31.2 ± 16.3	45.1 ± 20.7	**<0.0001**	**<0.0001**	**<0.0001**	**0.0003**
OPAS questionnaire							
Eye Pain Intensity for the last 24 h	0.1 ± 0.6	1.5 ± 3.5	7.8 ± 7.2	**<0.0001**	0.270	**<0.0001**	**<0.0001**
Eye Pain Intensity for the last 2 weeks	0.0 ± 0.3	1.7 ± 3.6	9.0 ± 7.7	**<0.0001**	0.188	**<0.0001**	**<0.0001**
Non-eye pain intensity	0.1 ± 0.7	0.1 ± 0.8	5.4 ± 7.1	**<0.0001**	0.999	**<0.0001**	**<0.0001**
QoL scores	0.1 ± 0.7	4.2 ± 10.3	23.8 ± 20.1	**<0.0001**	0.251	**<0.0001**	**<0.0001**
Aggravating Factors	0.1 ± 0.7	0.9 ± 3.1	4.9 ± 6.2	**<0.0001**	0.568	**<0.0001**	**<0.0001**
Associated Factors	0.1 ± 0.9	4.3 ± 9.5	12.2 ± 11.5	**<0.0001**	**0.040**	**<0.0001**	**<0.0001**

Table 3
Comparison of microneuroma and nerve parameters among 3 groups.

	Control	DED	NCP	*P* values	*P* values for post-hoc analysis		
					DED vs C	NCP vs C	NCP vs DED
Microneuroma parameters							
Frequency (%)	38/108 (35.2 %)	62/106 (58.5 %)	108/108 (100 %)	**<0.0001**	**0.001**	**<0.0001**	**<0.0001**
Number (n)	2.6 ± 2.1	2.7 ± 2.1	5.7 ± 3.5	**<0.0001**	>0.9999	**<0.0001**	**<0.0001**
Total area (μm^2)	439.1 ± 265.6	542.1 ± 344.1	1479.2 ± 1028.1	**<0.0001**	0.892	**<0.0001**	**<0.0001**
Total perimeter (μm)	233.4 ± 112.1	307.1 ± 196.5	740.3 ± 497.7	**<0.0001**	0.591	**<0.0001**	**<0.0001**
Average area (μm^2)	247.6 ± 140.5	263.3 ± 146.6	352.4 ± 246.7	**0.004**	0.926	**0.019**	**0.019**
Average perimeter (μm)	132.1 ± 52.2	133.0 ± 54.5	145.4 ± 63.5	0.300	0.997	0.460	0.386
Nerve parameters							
CNFD (fibers/mm^2)	14.4 ± 5.2	12.0 ± 5.3	12.5 ± 5.6	**0.005**	**0.006**	**0.036**	0.780
CNBD (fibers/mm^2)	13.8 ± 8.8	10.2 ± 7.4	11.3 ± 7.6	**0.006**	**0.002**	**0.033**	0.282
CNFL (mm/mm^2)	9.6 ± 2.6	8.0 ± 2.7	8.6 ± 2.7	**0.0001**	**<0.0001**	**0.016**	0.270
CTBD (branch points/mm^2)	23.9 ± 12.3	18.1 ± 9.5	19.4 ± 9.2	**0.0003**	**0.0003**	**0.006**	0.605
CNFA (mm^2/mm^2)	0.0045 ± 0.001	0.0038 ± 0.001	0.0042 ± 0.001	**0.002**	**0.0005**	0.175	**0.029**
CNFW (mm/mm^2)	0.0212 ± 0.001	0.0215 ± 0.001	0.0218 ± 0.001	**<0.0001**	**0.012**	**<0.0001**	**0.036**
CFracDim	1.41 ± 0.05	1.38 ± 0.05	1.40 ± 0.05	**<0.0001**	**<0.0001**	**0.017**	**0.027**

were observed between the OPAS scores of aggravating factors dimension and corneal nerve parameters CNFL (r = −0.37, P = 0.016), CNFD (r = -0.32, P = 0.037), as well as CFracDim (r = −0.35, P = 0.021). Further analysis revealed that CNFL and CFracDim had significant negative correlations with increased pain when exposed to wind, dry air, heat, or air conditioning (r = −0.33, P = 0.034; r = −0.32, P = 0.043, respectively, all P < 0.05).

When looking into the three types of NCP, we found that in peripheral NCP, both the total area and perimeter of MNs exhibited a significant positive correlation with eye pain intensity for the last 24 h (r = 0.55, P = 0.003; r = 0.57, P = 0.024, respectively; Fig. 4A and B). In terms of corneal nerve parameters, significant negative correlations were observed between the CNFL, CNFD, CFracDim and OPAS aggravating factors (r = −0.56, P = 0.022; r = −0.50, P = 0.043; and r = −0.56, P = 0.022, respectively; (Fig. 4C–E). No significant correlations were observed between these parameters in either the mixed or central NCP groups.

3.5. Potential imaging biomarkers for differentiating DED from NCP

As there are significant differences between the NCP and DED groups in the MN parameters, these parameters were included in the receiver-operating characteristic analysis. The AUC of MNs number for diagnosis of NCP was 0.871 (sensitivity: 81.1 %; specificity: 78.3 %). The AUC of MNs total area was 0.863 (sensitivity: 69.8 %; specificity: 85.9 %), and the AUC of MNs total perimeter was 0.864 (sensitivity: 76.4 %; specificity: 80.2 %). When these three parameters were combined, the AUC was 0.878, with a sensitivity of 82.1 % and specificity of 78.3 % (Table 6 and Fig. 4F).

Furthermore, we incorporated the OPAS items with the MN parameters. The AUC was improved to 0.910 (sensitivity: 79.4 %; specificity: 90.6 %) when combining the three MN parameters and Eye Pain Intensity for the last 2 weeks, and to 0.916 (sensitivity: 76.8 %; specificity 93.4 %) when combining the three MN parameters and 5 dimensions of the OPAS questionnaire on ocular symptoms (Table 6 and Fig. 4G).

3.6. Tear proteomic profiles and associated biological pathways

The plots of the PLS-DA analysis displayed a clear separation in the tear proteomic profiles between NCP and DED patients (Fig. 5A). A total of 129 significantly differentially expressed proteins were identified between the NCP and DED groups (Fig. 5B), with the top 20 significantly up-regulated or down-regulated tear proteins being shown in Table 7. Vinculin (VCL, $\log_2$FC = 1.17), which is involved in neuronal mechanosensing; myosin ID (MYO1D, $\log_2$FC = 1.12) which plays a role in the formation and/or maintenance of myelin; cytoplasmic FMR1 interacting protein 1 (CYFIP1, $\log_2$FC = 1.07), which is involved in neuronal activity, and ADP ribosylation factor guanine nucleotide exchange factor 1 (ARFGEF1, $\log_2$FC = 0.93) for neuro-inflammation, were significantly increased in NCP patients. On the other hand, DLG associated protein 4 (DLGAP4), which is involved in neuronal cell signaling and neuronal migration, was significantly decreased in the NCP group (log2FC = −1.84). Matrix metallopeptidase 9 (MMP9) and S100 calcium-binding protein A12 (S100A12) were significantly higher in DED patients ($\log_2$FC = −1.39 and $\log_2$FC = −1.02, respectively). On the pathway analysis, these significantly dysregulated proteins were related to immunological and inflammatory responses, regulation of neuron apoptotic process, regulation of translation at postsynapse, synaptic transmission, oxidative stress, and epithelial cell differentiation

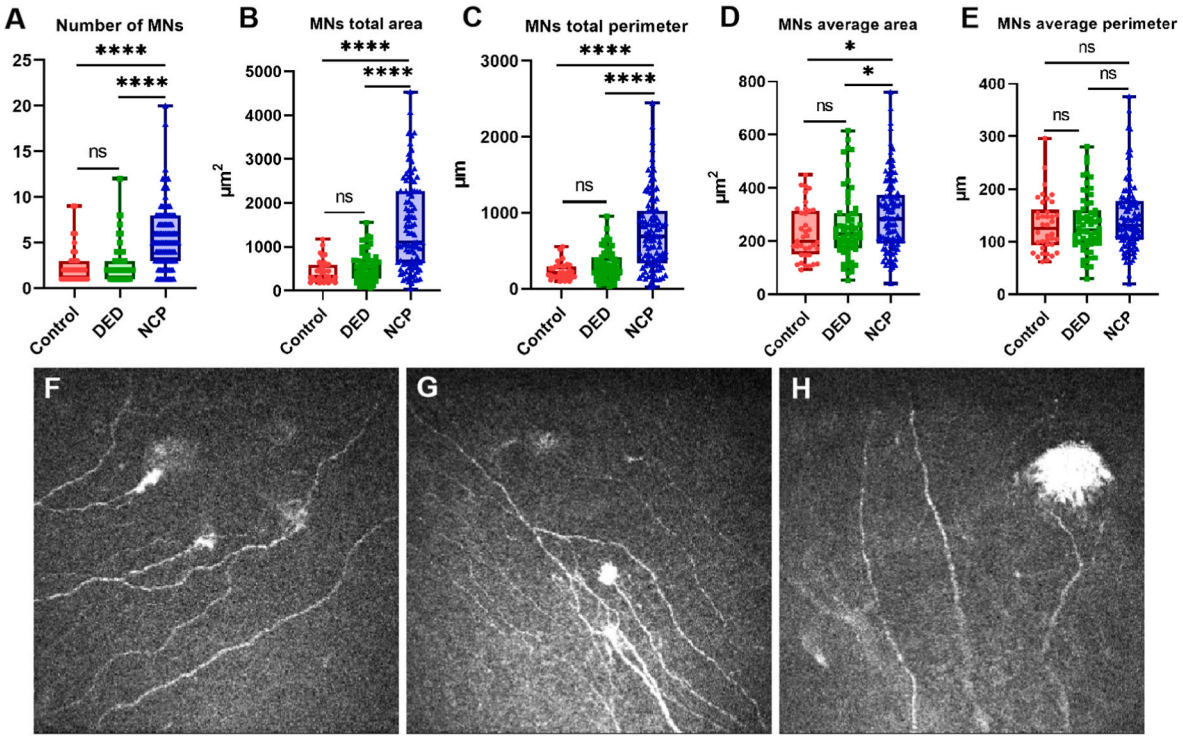

Fig. 1. Microneuromas (MNs) quantification and images in NCP, DED patients and controls. Comparison of MNs number (A), MNs total area (B), MNs total perimeter (C), MNs average area (D), MNs average perimeter (E); IVCM images of MNs in healthy controls (F), DED patients (G) and NCP patients (H) respectively. Error bars represent the standard error of the mean. $^{*}P < 0.05$, $^{****}P < 0.0001$. ns represents not statistically significant.

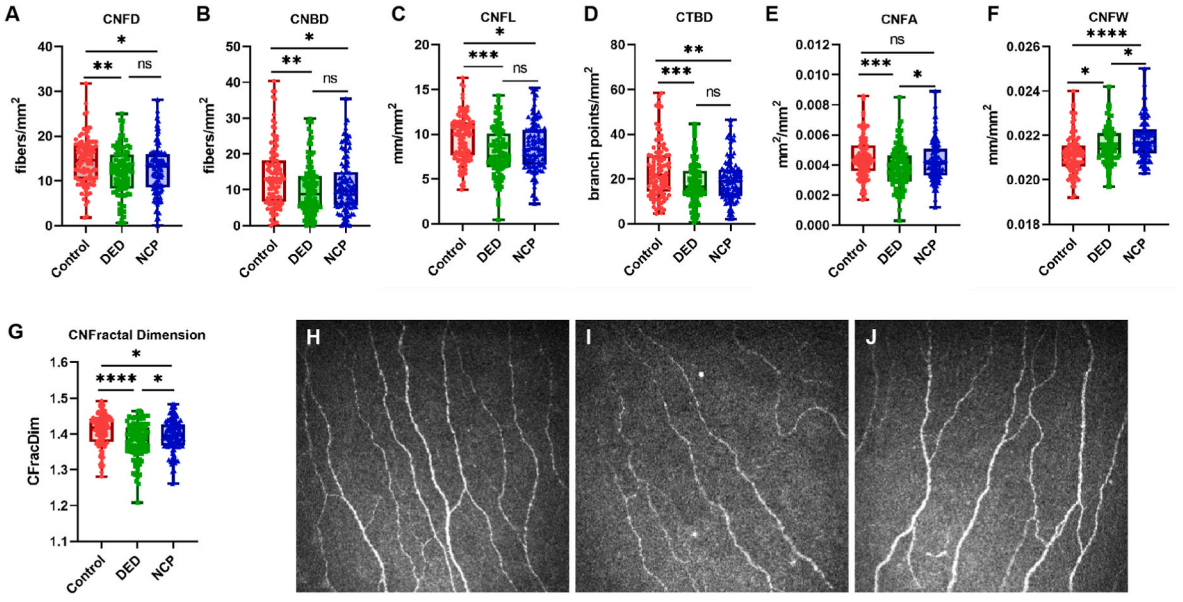

Fig. 2. Corneal nerve quantification and images in NCP, DED patients and controls: Comparison of CNFD (A), CNBD (B), CNFL (C), CTBD (D), CNFA (E), CNFW (F) and CFracDim (G). IVCM images of corneal nerves in healthy controls (H), DED patients (I) and NCP patients (J) respectively. Error bars represent the standard error of the mean. $^{*}P < 0.05$, $^{**}P < 0.01$, $^{***}P < 0.001$, $^{****}P < 0.0001$. ns represents not statistically significant.

(Fig. 5C).

4. Discussion

Currently, no objective imaging or molecular biomarkers are available to differentiate between NCP and DED. We compared the imaging characteristics, clinical features, and proteomic profiles between NCP and DED. We also found that patients' symptoms were positively correlated with MNs parameters, and the MN parameters help to differentiate NCP from DED. Additionally, the tear proteomics data serves as a valuable dataset for NCP and DED. These findings collectively provide important aspects in differentiating between NCP and DED, a challenge that has remained unmet in clinical practice.

We found that NCP patients had a higher percentage of systemic comorbidities. Insufficient sleep, persistent pain, and a decline in QoL may disrupt higher cognitive functions, leading to mood disorders.

Table 4
Comparison of corneal immune cell and epithelilal cell parameters among NCP, DED and control groups.

	Control	DED	NCP	*P* values	*P* values for post-hoc analysis		
					DED vs C	NCP vs C	NCP vs DED
Immune cell parameters							
Density (cells/μm^2)	0.021 ± 0.003	0.022 ± 0.002	0.022 ± 0.002	**0.003**	**0.003**	**0.018**	0.808
Average area(μm^2)	49.1 ± 7.7	45.4 ± 4.7	47.6 ± 7.4	**0.002**	**0.001**	0.486	**0.044**
Average length (μm)	11.8 ± 1.8	10.8 ± 0.8	11.2 ± 1.3	**<0.0001**	**0.0001**	0.078	**0.038**
Elongation (μm)	0.64 ± 0.06	0.62 ± 0.23	0.62 ± 0.06	**0.010**	**0.015**	**0.046**	0.994
Epithelial cell parameters							
Cell density (cells/μm^2)	0.0078 ± 0.0005	0.0083 ± 0.0007	0.0081 ± 0.0005	**<0.0001**	**<0.0001**	**0.015**	**0.019**
Average size (μm^2)	129.3 ± 9.2	121.3 ± 11.4	125.1 ± 8.1	**<0.0001**	**<0.0001**	**0.014**	**0.031**
Circularity	0.72 ± 0.01	0.71 ± 0.01	0.72 ± 0.02	0.083	0.173	0.969	0.101

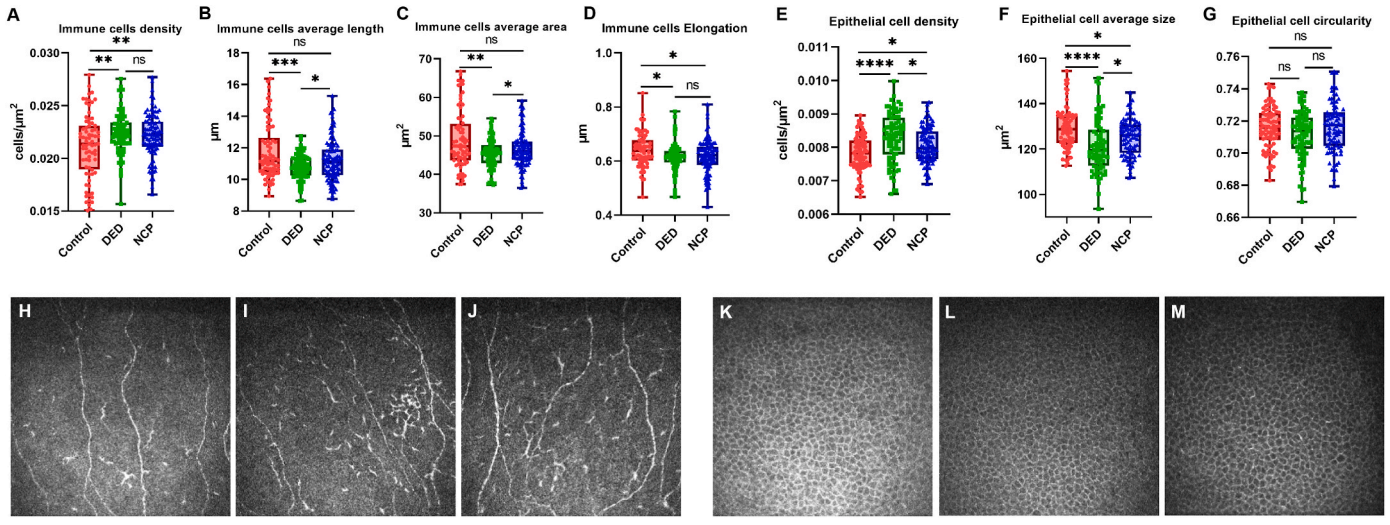

Fig. 3. Corneal immune cells and epithelial cell quantification and images in NCP, DED patients and controls: Comparison of immune cells density (A), immune cells average length (B), immune cells average area (C) and immune cells elongation (D); epithelial cell density (E), epithelial cell average size (F), and epithelial cell circularity (G). IVCM images of corneal immune cells in healthy controls (H), DED patients (I), NCP patients (J), corneal epithelial in healthy controls (K), DED patients (L) and NCP patients (M) respectively. Error bars represent the standard error of the mean. *$P < 0.05$, **$P < 0.01$, ***$P < 0.001$. ns represents not statistically significant.

Table 5
Correlations between imaging parameters and the scores of the OSDI and OPAS items in all participants.

		OSDI	Eye Pain Intensity for the last 24 h	Eye Pain Intensity for the last 2 weeks	QoL	Aggravating Factors	Associated Factors
MNs number	r	0.41	0.43	0.44	0.47	0.34	0.48
	P	**<0.0001**	**<0.0001**	**<0.0001**	**<0.0001**	**<0.0001**	**<0.0001**
MNs total area	r	0.44	0.42	0.42	0.43	0.29	0.43
	P	**<0.0001**	**<0.0001**	**<0.0001**	**<0.0001**	**<0.001**	**<0.0001**
MNs total perimeter	r	0.44	0.43	0.43	0.45	0.32	0.46
	P	**<0.0001**	**<0.0001**	**<0.0001**	**<0.0001**	**<0.0001**	**<0.0001**
MNs average area	r	0.32	0.30	0.33	0.32	0.20	0.30
	P	**<0.0001**	**<0.001**	**<0.0001**	**<0.0001**	**0.011**	**<0.001**
MNs average perimeter	r	0.27	0.26	0.26	0.25	0.21	0.25
	P	**0.001**	**0.001**	**0.001**	**0.002**	**0.007**	**0.002**
CNFD	r	−0.17	−0.09	−0.12	−0.04	−0.13	−0.06
	P	**0.028**	0.264	0.136	0.628	0.094	0.461
CNBD	r	−0.19	−0.08	−0.12	−0.02	−0.09	−0.03
	P	**0.015**	0.318	0.122	0.805	0.240	0.722
CNFL	r	−0.19	−0.07	−0.11	−0.01	−0.13	−0.03
	P	**0.018**	0.379	0.173	0.936	0.101	0.699
CTBD	r	−0.16	−0.06	−0.10	0.00	−0.07	0.01
	P	**0.040**	0.427	0.193	0.955	0.409	0.920
CNFA	r	−0.07	−0.03	−0.04	0.04	−0.07	0.03
	P	0.409	0.711	0.580	0.614	0.395	0.717
CNFW	r	0.19	0.14	0.19	0.13	0.07	0.20
	P	**0.017**	0.080	**0.017**	0.102	0.404	**0.014**
CFracDim	r	−0.18	−0.08	−0.13	−0.01	−0.12	−0.05
	P	**0.027**	0.291	0.112	0.854	0.121	0.541

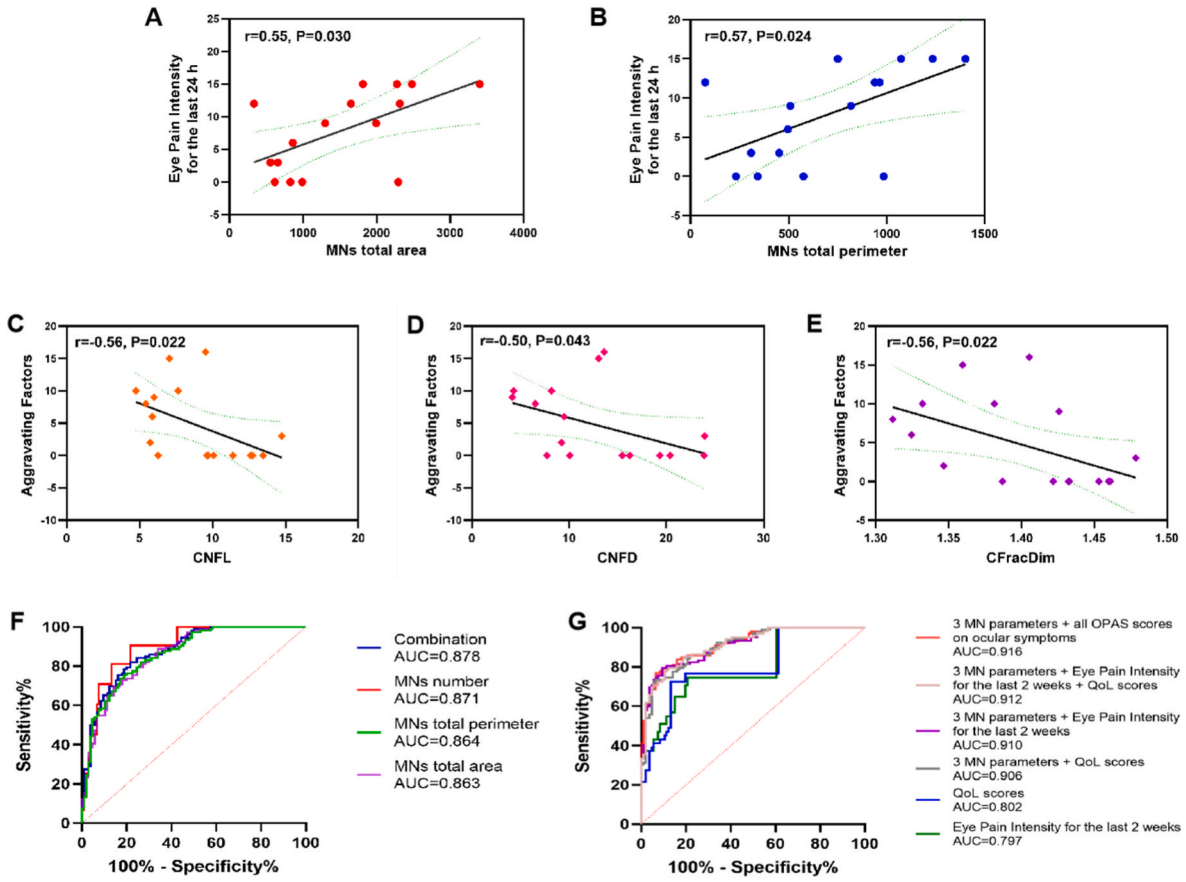

Fig. 4. Scatter plots and ROC curves. Scatter plots for the relationship between OPAS questionnaire eye pain intensity for the last 24h and MNs parameters in patients with peripheral NCP: MNs total area (A) and MNs total perimeter (B). Scatter plots for the relationship between OPAS questionnaire aggravating factors and corneal nerve parameters in patients with peripheral NCP: CNFL (C), CNFD (D), and CFracDim (E). Linear fitting was used as the analysis of R-squared values and residuals indicated that it was the most suitable model. ROC curves of the three MN parameters and their combination for differentiation NCP and DED (F); ROC curves of three MN parameters combined with OPAS scores for differentiation NCP and DED (G).

Table 6
Diagnostic efficacy for differentiation NCP and DED by MNs parameters and OPAS scores.

Evaluation parameters	AUC (95 %CI)	Cut-off value	Sensitivity	Specificity	Positive predictive value	Negative predictive value
MN parameters						
MNs number (n)	0.871 (0.824–0.918)	2.5	81.1 %	78.3 %	78.9 %	80.6 %
MNs total area (μm^2)	0.863 (0.816–0.911)	863	69.8 %	85.9 %	83.1 %	74.0 %
MNs total peremiter (μm)	0.864 (0.816–0.912)	365.5	76.4 %	80.2 %	80.2 %	77.5 %
Combination of 3 MN parameters	0.878 (0.833–0.923)	–	82.1 %	78.3 %	79.1 %	81.4 %
OPAS questionnaire						
Eye Pain Intensity for the last 2 weeks	0.797 (0.709–0.884)	1	74.5 %	79.3 %	78.7 %	76.9 %
QoL scores	0.802 (0.714–0.889)	6.5	72.6 %	86.8 %	84.9 %	77.2 %
Combination of 3 MN parameters + OPAS questionnaire						
3 MN parameters + Eye Pain Intensity for the last 2 weeks	0.910 (0.871–0.948)	–	81.4 %	83.0 %	83.0 %	83.0 %
3 MN parameters + QoL scores	0.906 (0.868–0.945)	–	81.4 %	80.2 %	80.7 %	82.5 %
3 MN parameters + Eye Pain Intensity for the last 2 weeks + QoL scores	0.912 (0.875–0.949)	–	82.4 %	82.1 %	82.4 %	83.7 %
3 MN parameters + all OPAS scores on ocular symptoms	0.916 (0.880–0.953)	–	83.8 %	83.0 %	83.4 %	85.1 %

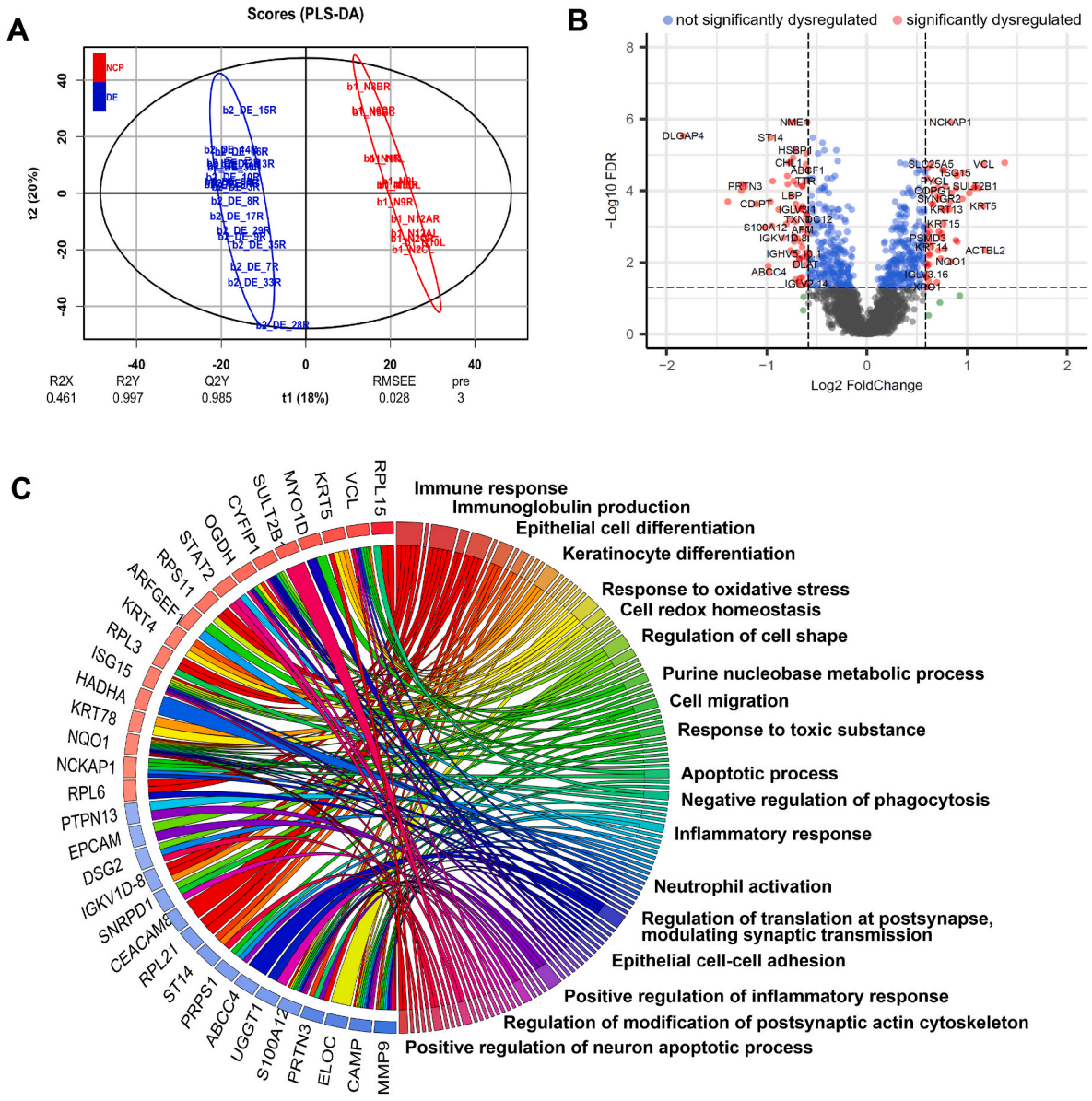

Fig. 5. Tear proteomic profiles of NCP patients and DED patients. Partial Least Squares Discrimination Analysis (PLS-DA) analysis showing a clear separation of the tear proteomic profiles of the NCP patients versus DED patients (A). Volcano plots presenting the fold changes (FC) of the tear proteins comparing NCP patients versus DED patients, red: significantly dysregulated, blue: not significantly dysregulated (B). Chord plot demonstrating GO analysis of top 20 up and down-regulated proteins and associated pathways in NCP group in comparison to the DED group (C). Significantly up-regulated (FC > 1.5 and P < 0.05, i.e. $\log_2$FC > 0.58) and down-regulated (FC < 0.67 and P < 0.05, i.e. $\log_2$FC < −0.58) proteins are shown. (For interpretation of the references to colour in this figure legend, the reader is referred to the Web version of this article.)

These negative emotions further intensify the experience of NCP, exacerbating pain symptoms [40]. Our group previously reported that NCP is significantly more debilitating than DED in all aspects of QoL [2].

The corneal nerves stimulate the tear reflex, activating the efferent corneal nerves in the production of the tear film [41]. The abnormal nerve function in NCP patients leads to the impairment of tear reflex and neural nutritional effect, resulting in decreased tear production and stability. Additionally, the TBUT and ocular surface staining were the worst in the DED patients, highlighting the unstable tear film and disruptive ocular surface tight junctions.

The appearance and frequency of MNs have been a subject of research interest in NCP. There are several hyper-reflective physiological or pathological structures to be distinguished from MNs on IVCM. MNs typically present with bulges, varicosities, tangles, or hyper-reflective sites connecting to axons, while corneal stromal-epithelial nerve penetration sites (CSENPS) are mainly hyper-reflective but diffuse patterns associated with branch points and continuous with a stromal nerve trunk [42] (Supplementary Fig. 1). Other corneal hyper-reflectivities, such as irregular tear film, subepithelial fibrous reticular tissue, and the aggregation and infiltration of immune cells, could be also seen on IVCM images (Supplementary Fig. 2). However, these structures would not connected to nerves or axons and could be differentiated from corneal MNs. Our analysis revealed a significant increase in the number and size of MNs in NCP than in DED and controls. This suggests that MNs may serve as a pathological basis for NCP. We further demonstrated that MN parameters serve as highly effective biomarkers for distinguishing NCP from DED with an AUC of 0.863–0.878. When we further identify the cut-off values, the number of MNs >2.5, the total area of MNs >863 μm^2, and the total perimeter of MNs >365.5 μm, as well as the presence of eye pain (i.e. pain score >1) in the past two weeks, can be used as sensitive indicators for the diagnosis of NCP. In clinical practice, it suggests that 91.6 % of NCP patients

Table 7
Top 20 Significantly Up-regulated or Down-regulated Tear Proteins in Patients with NCP compared to DED.

Up-regulated proteins	Protein name	Log2 FC	P value	Down-regulated proteins	Protein name	Log2 FC	P value
1	Ribosomal protein L15(RPL15)	1.375	<0.001	1	DLG associated protein 4 (DLGAP4)	−1.836	<0.001
2	Vinculin(VCL)	1.165	<0.001	2	Matrix Metallopeptidase 9 (MMP9)	−1.389	<0.001
3	keratin 5 (KRT5)	1.161	<0.001	3	Cathelicidin antimicrobial peptide (CAMP)	−1.254	<0.001
4	Myosin ID (MYO1D)	1.119	<0.001	4	Elongin C (ELOC)	−1.250	<0.001
5	Sulfotransferase family 2B member 1(SULT2B1)	1.079	<0.001	5	Proteinase 3 (PRTN3)	−1.217	<0.001
6	Cytoplasmic FMR1 interacting protein 1(CYFIP1)	1.068	<0.001	6	S100 calcium binding protein A12 (S100A12)	−1.020	<0.001
7	Oxoglutarate dehydrogenase (OGDH)	1.021	<0.001	7	ATP binding cassette subfamily C member 4 (PEL blood group) (ABCC4)	−0.978	0.004
8	ADP ribosylation factor guanine nucleotide exchange factor 1(ARFGEF1)	0.927	0.030	8	Phosphoribosyl pyrophosphate synthetase 1(PRPS1)	−0.963	<0.001
9	Hydroxyacyl-CoA dehydrogenase trifunctional multienzyme complex subunit alpha(HADHA)	0.890	<0.001	9	CEA cell adhesion molecule 8 (CEACAM8)	−0.942	<0.001
10	NAD(P)H quinone dehydrogenase 1(NQO1)	0.838	0.002	10	Desmoglein 2 (DSG2)	−0.795	<0.001

can be accurately diagnosed by assessing the MNs and asking patients if they experienced eye pain for the past 2 weeks. This approach for the first time reported clinically practical imaging references for NCP diagnosis.

Our study also identified the presence of corneal MNs in controls and DED patients, which is in agreement with previous studies where MNs were observed in asymptomatic young individuals and various ocular surface diseases [17,30,43,44]. The frequency of MNs was higher in the DED group than in the controls. We also found that all five dimensions of OPAS scores exhibited significant and positive correlations with the number, total area, and total perimeter of MNs. Additionally, these MN parameters were positively correlated with the OSDI scores. When there is insult in corneal nerves, the injured region is initially colonized by regenerating healthy nerve fibers, followed by the reinnervation of damaged axons and development of MNs [45]. MNs are believed to be the source of spontaneous and aberrant firing, leading to hyperalgesia and abnormal pain in response to noxious stimuli [45,46]. MNs also induce spontaneous abnormal electrical activity in corneal nerve C fibers, transmitting pain sensations. All these led to patients' symptoms as evaluated by the OPAS and OSDI.

In the present study, significantly worse corneal nerve metrics were observed in the NCP and DED patients compared to controls. When comparing the NCP with the DED group, we noted significantly lower CFracDim in the DED group, suggesting a more compromised nerve distribution. The mean CNFW was highest in the NCP group, possibly due to underlying neuroinflammation. Neuroinflammation triggers compensatory release of neurotrophic factors, leading to hypertrophy of the nerves. Our previous studies have shown a significant elevation in the tear NGF concentrations in NCP patients [9]. In this study, we also identified several proteins linked to neuroinflammation that were significantly upregulated in the NCP group, which may also contribute to the nerve swelling.

Furthermore, we found that hyperalgesia was significantly correlated with the CNFL, CNFD, and CFracDim, particularly in the peripheral NCP patients where a higher correlation was observed. Similarly, in a study on patients with corneal neuropathy and photoallodynia, a significant negative correlation was found between photoallodynia symptom severity and total nerve density [47].

Our study observed a significantly higher number of MNs in peripheral and mixed NCP than in central NCP. This finding aligns with the previously reported results where the authors demonstrated a significantly higher number of MNs among individuals responsive to topical anesthetics than non-responsive individuals [5]. Our study also showed the total area and perimeter of MNs were significantly correlated with the eye pain score within the past 24 h in peripheral NCP, whereas no such correlation was observed in mixed or central NCP. These suggest that peripheral NCP is primarily associated with corneal nerve damage and abnormal repair processes, highlighting the potential use of the changes of the MN number and size to evaluate treatment effectiveness.

Our findings demonstrate a significantly higher immune cells density and more mature immune cells activities in the DED and NCP groups compared to the controls. Under neuroinflammatory stimulation and increased levels of corneal chemokines/cytokines, the number of corneal immune cells increases, partly by recruiting immune cells precursors from the blood [48]. Furthermore, the maturity of corneal immune cells remains a subject of ongoing discussion [16,49]. Mature immune cells exhibited larger sizes, longer dendrites, and faster migration rates in response to neuroinflammation, while immature immune cells appeared rounder with shorter dendrites [50]. Yu et al. [51] proposed that corneal immune cells can establish links with neurons through dendrites, and mature immune cells seem to stabilize newly formed nerve endings and guide nerve regeneration. Additionally, we found that the immune cells density and elongation were not different between NCP and DED, suggesting that immune cells parameters may not be good differentiating factors for NCP and DED.

Hypertonicity and inflammation stimulate apoptosis in the corneal epithelial cells [52]. In our IVCM analysis, the DED group exhibited significantly higher epithelial cell density and smaller cells, potentially attributed to the increased apoptosis and compensatory proliferative ability of basal epithelial cells. Another research also reported a significant increase in the corneal epithelial cell density in DED [53]. The density and size of the epithelial cells in NCP patients were between those observed in DED patients and controls, suggesting less corneal apoptotic activities compared to DED patients, which could explain the milder corneal staining observed in the NCP group.

In the tear proteomic analysis, several proteins were significantly upregulated in NCP than DED. VCL is a key regulator of neuronal mechanosensing, modulating neuronal regeneration [54]. CYFIP1 is involved in neuronal activity, and its overexpression results in a reduction in the neurite length [55]. Up-regulated ARFGEF1 implies neurite outgrowth, initiation of myelination, and neuroinflammation [56], while a neuroprotective protein DLGAP4 was down-regulated in the NCP group. Conversely, inflammatory proteins, such as MMP9 and S100A12 were significantly upregulated in DED patients. Increased MMP9 activity on the ocular surface amplifies the chronic inflammation of dry eye [57], and S100A has been shown to play a role in ocular surface inflammatory diseases [58].

Several pathways linked to the abovementioned proteins were identified. The regulation of neuron apoptosis and modulation of synaptic transmission were up-regulated in NCP patients. The former was reported in the neuropathic pain with chronic constriction injury of sciatic nerves [59]. The latter involves in spinal postsynaptic potentiation and chronic pain [60]. Immunological and inflammatory responses, epithelial cell-cell, and neutrophil interactions were increased in DED

patients, suggesting that mucosal immune responses play roles in the development and progression in DED [61].

There are several limitations in the present study. This was a cross-sectional study, as we aimed to compare the imaging and protein characteristics of NCP and DED patients. The causal effects can not be determined. Some DED or NCP patients have received treatments such as topical cyclosporin before referral, which may affect immune cells analysis. However, our data reflects the real-world clinical practice. DED and NCP may coexist, or one may be a precursor or a sequel. However, we used the established diagnostic criteria for our study as the ground truth. The data of corneal sensitivity data were not included in this work, as the study was retrospective, and corneal sensitivity evaluation is not a routine test in our DED clinics. It can be included in future work.

In conclusion, we described the differential characteristics in the clinical manifestations, imaging features, and tear proteomic between NCP and DED. Furthermore, the differential proteins we identified provide a better understanding of the pathophysiology between NCP and DED in the molecular aspect. It may also contribute to exploring novel biomarkers and new therapeutic targets for NCP. Although NCP and DED are not mutually exclusive, our multi-modal data offers more in-depth insight into NCP and DED, two common ocular surface diseases encountered in daily practice.

CRediT authorship contribution statement

Jun Cheng: Writing – review & editing, Writing – original draft. **Chang Liu:** Data curation. **Mingyi Yu:** Data curation. **Isabelle Xin Yu Lee:** Data curation. **Xinyue Wang:** Formal analysis. **Victor Wei-Tse Hsu:** Formal analysis. **Aya Takahashi:** Data curation. **Jodhbir S. Mehta:** Writing – review & editing. **Lei Zhou:** Formal analysis. **Louis Tong:** Writing – review & editing, Conceptualization. **Yu-Chi Liu:** Writing – review & editing, Investigation, Funding acquisition, Data curation, Conceptualization.

Funding

This work was supported by Clinician Scientist Award Grant from the Singapore National Medical Research Council (MOH-CSAINV21jun-0001); National Natural Science Foundation of China (Grant No. 82301180); Project ZR2022MH105 supported by Shandong Provincial Natural Science Foundation; Young Elite Sponsorship Program of Shandong Provincial Medical Association.

Declaration of competing interest

The authors have no financial or proprietary interest in the materials presented herein.

Acknowledgement

LZ would like to thank the support from the InnoHK initiative of the Innovation and Technology Commission of the Hong Kong Special Administrative Region Government and the Hong Kong Polytechnic University grant (P0043882), Singapore National Medical Research Council: Clinician Scientist Individual Research Grant (CIRG24jul-0010) and Clinician Scientist Awards (CSAINV24jul-0005).

Appendix A. Supplementary data

Supplementary data to this article can be found online at https://doi.org/10.1016/j.jtos.2025.08.002.

References

[1] Finnerup NB, Kuner R, Jensen TS. Neuropathic pain: from mechanisms to treatment. Physiol Rev 2021 Jan 1;101(1):259–301. https://doi.org/10.1152/physrev.00045.2019.
[2] Chin JY, Tong L, Liu C, Lee IXY, Wong JHF, Wong RKT, Mehta JS, Liu YC. Quality of life and symptomatology in neuropathic corneal pain in comparison with dry eye syndrome. Cornea 2024. https://doi.org/10.1097/ICO.0000000000003674.
[3] Leonardi A, Feuerman OM, Salami E, Lazzarini D, Cavarzeran F, Freo U, Maggioni F. Coexistence of neuropathic corneal pain, corneal nerve abnormalities, depression, and low quality of life. Eye (London, England) 2024;38(3):499–506. https://doi.org/10.1038/s41433-023-02710-w.
[4] Goyal S, Hamrah P. Understanding neuropathic corneal Pain–Gaps and current therapeutic approaches. Semin Ophthalmol 2016;31(1–2):59–70. https://doi.org/10.3109/08820538.2015.1114853.
[5] Wong NSQ, Liu C, Lin MT, Lee IXY, Tong L, Liu YC. Neuropathic corneal pain after coronavirus disease 2019 (COVID-19) infection. Diseases 2024;12(2):37. https://doi.org/10.3390/diseases12020037.
[6] Mansoor H, Tan HC, Lin MT, Mehta JS, Liu YC. Diabetic corneal neuropathy. J Clin Med 2020;9(12):3956. https://doi.org/10.3390/jcm9123956.
[7] Ross AR, Al-Aqaba MA, Almaazmi A, Messina M, Nubile M, Mastropasqua L, Dua HS, Said DG. Clinical and in vivo confocal microscopic features of neuropathic corneal pain. Br J Ophthalmol 2020;104(6):768–75. https://doi.org/10.1136/bjophthalmol-2019-314799.
[8] Moein HR, Akhlaq A, Dieckmann G, Abbouda A, Pondelis N, Salem Z, Müller RT, Cruzat A, Cavalcanti BM, Jamali A, Hamrah P. Visualization of microneuromas by using in vivo confocal microscopy: an objective biomarker for the diagnosis of neuropathic corneal pain? Ocul Surf 2020;18(4):651–6. https://doi.org/10.1016/j.jtos.2020.07.004.
[9] Yawata N, Selva KJ, Liu YC, Tan KP, Lee AWL, Siak J, Lan W, Vania M, Arundhati A, Tong L, Li J. Dynamic change in natural killer cell type in the human ocular mucosa in situ as means of immune evasion by adenovirus infection. Mucosal Immunol. 2016;9(1):159–70. https://doi.org/10.1038/mi.2015.47.
[10] Skaper SD, Facci L, Giusti P. Mast cells, glia and neuroinflammation: partners in crime? Immunology 2014;141(3):314–27. https://doi.org/10.1111/imm.12170.
[11] Patel S, Mittal R, Sarantopoulos KD, Galor A. Neuropathic ocular surface pain: emerging drug targets and therapeutic implications. Expert Opin Ther Targets 2022;26(8):681–95. https://doi.org/10.1080/14728222.2022.2122438.
[12] Kalangara JP, Galor A, Levitt RC, Covington DB, McManus KT, Sarantopoulos CD, Felix ER. Characteristics of ocular pain complaints in patients with idiopathic dry eye symptoms. Eye Contact Lens 2017;43(3):192–8. https://doi.org/10.1097/ICL.0000000000000249.
[13] Labbé A, Alalwani H, Van Went C, Brasnu E, Georgescu D, Baudouin C. The relationship between subbasal nerve morphology and corneal sensation in ocular surface disease. Investig Ophthalmol Vis Sci 2012;53(8):4926–31. https://doi.org/10.1167/iovs.11-8708.
[14] Labbé A, Liang Q, Wang Z, Zhang Y, Xu L, Baudouin C, Sun X. Corneal nerve structure and function in patients with non-sjogren dry eye: clinical correlations. Investig Ophthalmol Vis Sci 2013;54(8):5144–50. https://doi.org/10.1167/iovs.13-12370.
[15] Dermer H, Hwang J, Mittal R, Cohen AK, Galor A. Corneal sub-basal nerve plexus microneuromas in individuals with and without dry eye. Br J Ophthalmol 2022;106(5):616–22. https://doi.org/10.1136/bjophthalmol-2020-317891.
[16] Tuisku IS, Konttinen YT, Konttinen LM, Tervo TM. Alterations in corneal sensitivity and nerve morphology in patients with primary Sjögren's syndrome. Exp Eye Res 2008;86(6):879–85. https://doi.org/10.1016/j.exer.2008.03.002.
[17] Tepelus TC, Chiu GB, Huang J, Huang P, Sadda SR, Irvine J, Lee OL. Correlation between corneal innervation and inflammation evaluated with confocal microscopy and symptomatology in patients with dry eye syndromes: a preliminary study. Graefe's archive for clinical and experimental ophthalmology = Albrecht von Graefes Archiv fur klinische und experimentelle Ophthalmologie 2017;255(9):1771–8. https://doi.org/10.1007/s00417-017-3680-3.
[18] Aggarwal S, Kheirkhah A, Cavalcanti BM, Cruzat A, Jamali A, Hamrah P. Correlation of corneal immune cell changes with clinical severity in dry eye disease: an in vivo confocal microscopy study. Ocul Surf 2021;19:183–9. https://doi.org/10.1016/j.jtos.2020.05.012.
[19] Enríquez-de-Salamanca A, Castellanos E, Stern ME, Fernández I, Carreño E, García-Vázquez C, Herreras JM, Calonge M. Tear cytokine and chemokine analysis and clinical correlations in evaporative-type dry eye disease. Mol Vis 2010;16:862–73.
[20] Asiedu K. Role of ocular surface neurobiology in neuronal-mediated inflammation in dry eye disease. Neuropeptides 2022;95:102266. https://doi.org/10.1016/j.npep.2022.102266.
[21] Ames P, Galor A. Cyclosporine ophthalmic emulsions for the treatment of dry eye: a review of the clinical evidence. Clin Invest 2015;5(3):267–85. https://doi.org/10.4155/cli.14.135.
[22] Holland EJ, Luchs J, Karpecki PM, Nichols KK, Jackson MA, Sall K, Tauber J, Roy M, Raychaudhuri A, Shojaei A. Lifitegrast for the treatment of dry eye disease: results of a phase III, randomized, double-masked, placebo-controlled trial (OPUS-3). Ophthalmology 2017;124(1):53–60. https://doi.org/10.1016/j.ophtha.2016.09.025.
[23] Anam A, Liu C, Tong L, Liu YC. Blood-Derived eye drops for the treatment of corneal neuropathic pain. J Ocul Pharmacol Therapeut 2024 Jun;40(5):281–92. https://doi.org/10.1089/jop.2023.0155.
[24] Dieckmann G, Ozmen MC, Cox SM, Engert RC, Hamrah P. Low-dose naltrexone is effective and well-tolerated for modulating symptoms in patients with neuropathic

corneal pain. Ocul Surf 2021;20:33–8. https://doi.org/10.1016/j.jtos.2020.12.003.
[25] Kannan R, Das S, Shetty R, Zhou L, Ghosh A, Deshpande V. Tear proteomics in dry eye disease. Indian J Ophthalmol 2023;71(4):1203–14. https://doi.org/10.4103/IJO.IJO_2851_22.
[26] Teo CHY, Liu C, Lee IXY, Lin MT, Liu F, Toh CJL, Koh SK, Lu DQ, Lam TC, Zhou L, Tong L, Mehta JS, Liu YC. Neuropathic corneal pain following refractive surgery: risk factors, clinical manifestations, imaging and proteomic characteristics. The British journal of ophthalmology. Advance online publication; 2025. https://doi.org/10.1136/bjo-2024-325996. bjo-2024-325996.
[27] Sall K, Foulks GN, Pucker AD, Ice KL, Zink RC, Magrath G. Validation of a modified national eye institute grading scale for corneal fluorescein staining. Clin Ophthalmol 2023;17:757–67. https://doi.org/10.2147/OPTH.S398843.
[28] Wolffsohn JS, Arita R, Chalmers R, Djalilian A, Dogru M, Dumbleton K, Gupta PK, Karpecki P, Lazreg S, Pult H, Sullivan BD, Tomlinson A, Tong L, Villani E, Yoon KC, Jones L, Craig JP. TFOS DEWS II diagnostic methodology report. Ocul Surf 2017;15(3):539–74. https://doi.org/10.1016/j.jtos.2017.05.001.
[29] Liu YC, Jung ASJ, Chin JY, Yang LWY, Mehta JS. Cross-sectional study on corneal denervation in contralateral eyes following SMILE versus LASIK. J Refract Surg 2020;36(10):653–60. https://doi.org/10.3928/1081597X-20200730-01.
[30] Toh CJL, Liu C, Lee IXY, Yu Lin MT, Tong L, Liu YC. Clinical associations of corneal neuromas with ocular surface diseases. Neural Regeneration Res 2024;19(1):140–7. https://doi.org/10.4103/1673-5374.375308.
[31] Liu F, Liu C, Lee IXY, Lin MTY, Liu YC. Corneal dendritic cells in diabetes mellitus: a narrative review. Front Endocrinol 2023;14:1078660. https://doi.org/10.3389/fendo.2023.1078660.
[32] Teo CHY, Ong HS, Liu YC, Tong L. Meibomian gland dysfunction is the primary determinant of dry eye symptoms: analysis of 2346 patients. Ocul Surf 2020;18(4):604–12. https://doi.org/10.1016/j.jtos.2020.06.008.
[33] Bron AJ, Evans VE, Smith JA. Grading of corneal and conjunctival staining in the context of other dry eye tests. Cornea 2003;22(7):640–50. https://doi.org/10.1097/00003226-200310000-00008.
[34] Lemp MA. Report of the national eye Institute/Industry workshop on clinical trials in dry eyes. CLAO J : Official Pub Contact Lens Assoc Ophthalmologists, Inc 1995;21(4):221–32.
[35] Schiffman RM, Christianson MD, Jacobsen G, Hirsch JD, Reis BL. Reliability and validity of the ocular surface disease index. Arch Ophthalmol 2000;118(5):615–21. https://doi.org/10.1001/archopht.118.5.615. Chicago, Ill. : 1960.
[36] Qazi Y, Hurwitz S, Khan S, Jurkunas UV, Dana R, Hamrah P. Validity and reliability of a Novel Ocular Pain Assessment Survey (OPAS) in quantifying and monitoring corneal and ocular surface pain. Ophthalmology 2016;123(7):1458–68. https://doi.org/10.1016/j.ophtha.2016.03.006.
[37] Teo CHY, Lin MT, Lee IXY, Koh SK, Zhou L, Goh DS, Choi H, Koh HWL, Lam AYR, Lim PS, Mehta JS, Kovalik JP, Coffman TM, Tan HC, Liu YC. Oral peroxisome proliferator-activated Receptor-α agonist enhances corneal nerve regeneration in patients with type 2 diabetes. Diabetes 2023;72(7):932–46. https://doi.org/10.2337/db22-0611.
[38] Liu YC, Yam GH, Lin MT, Teo E, Koh SK, Deng L, Zhou L, Tong L, Mehta JS. Comparison of tear proteomic and neuromediator profiles changes between small incision lenticule extraction (SMILE) and femtosecond laser-assisted in-situ keratomileusis (LASIK). J Adv Res 2020;29:67–81. https://doi.org/10.1016/j.jare.2020.11.001.
[39] Hanley JA, McNeil BJ. The meaning and use of the area under a receiver operating characteristic (ROC) curve. Radiology 1982;143(1):29–36. https://doi.org/10.1148/radiology.143.1.7063747.
[40] Vandekerckhove M, Wang YL. Emotion, emotion regulation and sleep: an intimate relationship. AIMS Neurosci 2017;5(1):1–17. https://doi.org/10.3934/Neuroscience.2018.1.1.
[41] Lasagni Vitar RM, Rama P, Ferrari G. The two-faced effects of nerves and neuropeptides in corneal diseases. Prog Retin Eye Res 2022;86:100974. https://doi.org/10.1016/j.preteyeres.2021.100974.
[42] Stepp MA, Pal-Ghosh S, Downie LE, Zhang AC, Chinnery HR, Machet J, Di Girolamo N. Corneal epithelial "Neuromas": a case of mistaken identity? Cornea 2020;39(7):930–4. https://doi.org/10.1097/ICO.0000000000002294.
[43] D'Souza S, Shetty R, Nair AP, Agrawal R, Dickman MM, Khamar P, Nuijts RMMA, Ghosh A, Sethu S. Corneal confocal microscopy features and tear molecular profile in study participants with discordance between ocular surface disease clinical signs and discomfort. J Clin Med 2022;11(9):2407. https://doi.org/10.3390/jcm11092407.
[44] Guerrero-Moreno A, Liang H, Moreau N, Luzu J, Rabut G, Melik Parsadaniantz S, Labbé A, Baudouin C, Réaux-Le Goazigo A. Corneal nerve abnormalities in painful dry eye disease patients. Biomedicines 2021;9(10):1424. https://doi.org/10.3390/biomedicines9101424.
[45] Belmonte C, Acosta MC, Gallar J. Neural basis of sensation in intact and injured corneas. Exp Eye Res 2004;78(3):513–25. https://doi.org/10.1016/j.exer.2003.09.023.
[46] Sim R, Yong K, Liu YC, Tong L. In vivo confocal microscopy in different types of dry eye and meibomian gland dysfunction. J Clin Med 2022;11(9):2349. https://doi.org/10.3390/jcm11092349.
[47] Aggarwal S, Kheirkhah A, Cavalcanti BM, Cruzat A, Colon C, Brown E, Borsook D, Prüss H, Hamrah P. Autologous serum tears for treatment of photoallodynia in patients with corneal neuropathy: efficacy and evaluation with in vivo confocal microscopy. Ocul Surf 2015;13(3):250–62. https://doi.org/10.1016/j.jtos.2015.01.005.
[48] Jamali A, Seyed-Razavi Y, Chao C, Ortiz G, Kenyon B, Blanco T, Harris DL, Hamrah P. Intravital multiphoton microscopy of the ocular surface: alterations in conventional dendritic cell morphology and kinetics in dry eye disease. Front Immunol 2020;11:742. https://doi.org/10.3389/fimmu.2020.00742.
[49] Kheirkhah A, Rahimi Darabad R, Cruzat A, Hajrasouliha AR, Witkin D, Wong N, Dana R, Hamrah P. Corneal epithelial immune dendritic cell alterations in subtypes of dry eye disease: a pilot in vivo confocal microscopic study. Investig Ophthalmol Vis Sci 2015;56(12):7179–85. https://doi.org/10.1167/iovs.15-17433.
[50] Blanco P, Palucka AK, Pascual V, Banchereau J. Dendritic cells and cytokines in human inflammatory and autoimmune diseases. Cytokine Growth Factor Rev 2008;19(1):41–52. https://doi.org/10.1016/j.cytogfr.2007.10.004.
[51] Yu FX, Lee PSY, Yang L, Gao N, Zhang Y, Ljubimov AV, Yang E, Zhou Q, Xie L. The impact of sensory neuropathy and inflammation on epithelial wound healing in diabetic corneas. Prog Retin Eye Res 2022;89:101039. https://doi.org/10.1016/j.preteyeres.2021.101039.
[52] López-Cano JJ, González-Cela-Casamayor MA, Andrés-Guerrero V, Herrero-Vanrell R, Benítez-Del-Castillo JM, Molina-Martínez IT. Combined hyperosmolarity and inflammatory conditions in stressed human corneal epithelial cells and macrophages to evaluate osmoprotective agents as potential DED treatments. Exp Eye Res 2021;211:108723. https://doi.org/10.1016/j.exer.2021.108723.
[53] Kasikci M, Erogul O, Polat O. Evaluation of aqueous-deficient and evaporative dry eye cases with confocal microscopy. J Fr Ophtalmol 2023;46(10):1161–8. https://doi.org/10.1016/j.jfo.2023.05.024.
[54] Wang DY, Melero C, Albaraky A, Atherton P, Jansen KA, Dimitracopoulos A, Dajas-Bailador F, Reid A, Franze K, Ballestrem C. Vinculin is required for neuronal mechanosensing but not for axon outgrowth. Exp Cell Res 2021;407(2):112805. https://doi.org/10.1016/j.yexcr.2021.112805.
[55] Oguro-Ando A, Rosensweig C, Herman E, Nishimura Y, Werling D, Bill BR, Berg JM, Gao F, Coppola G, Abrahams BS, Geschwind DH. Increased CYFIP1 dosage alters cellular and dendritic morphology and dysregulates mTOR. Mol Psychiatr 2015;20(9):1069–78. https://doi.org/10.1038/mp.2014.124.
[56] You Z, Yang Z, Cao S, Deng S, Chen Y. The novel KLF4/BIG1 regulates LPS-mediated neuro-inflammation and migration in BV2 cells via PI3K/Akt/NF-kB signaling pathway. Neuroscience 2022;488:102–11. https://doi.org/10.1016/j.neuroscience.2022.01.014.
[57] So HR, Baek J, Lee JY, Kim HS, Kim MS, Kim EC. Comparison of matrix metallopeptidase-9 expression following cyclosporine and diquafosol treatment in dry eye. Ann Med 2023;55(1):2228192. https://doi.org/10.1080/07853890.2023.2228192.
[58] Tong L, Lan W, Lim RR, Chaurasia SS. S100A proteins as molecular targets in the ocular surface inflammatory diseases. Ocul Surf 2014;12(1):23–31. https://doi.org/10.1016/j.jtos.2013.10.001.
[59] Wu F, Miao X, Chen J, Sun Y, Liu Z, Tao Y, Yu W. Down-regulation of GAP-43 by inhibition of caspases-3 in a rat model of neuropathic pain. Int J Clin Exp Pathol 2012;5(9):948–55.
[60] Xie RG, Chu WG, Liu DL, Wang X, Ma SB, Wang F, Wang FD, Lin Z, Wu WB, Lu N, Liu YY, Han WJ, Zhang H, Bai ZT, Hu SJ, Tao HR, Kuner T, Zhang X, Kuner R, Wu SX, Luo C. Presynaptic NMDARs on spinal nociceptor terminals state-dependently modulate synaptic transmission and pain. Nat Commun 2022;13(1):728. https://doi.org/10.1038/s41467-022-28429-y.
[61] Liu Z, Xie H, Li L, Jiang D, Qian Y, Zhu X, Dai M, Li Y, Wei R, Luo Z, Xu W, Zheng Q, Shen J, Zhou M, Zeng W, Chen W. Single-cell landscape reveals the epithelial cell-centric pro-inflammatory immune microenvironment in dry eye development. Mucosal Immunol 2024;17(3):491–507. https://doi.org/10.1016/j.mucimm.2023.11.008.